Chinese Chemical Letters 32 (2021) 1691–1695

Contents lists available at ScienceDirect

Chinese Chemical Letters

journal homepage: www.elsevier.com/locate/cclet

Communication

Conformational effect on fluorescence emission of tetraphenylethylene-based metallacycles

Zhewen Guo[a], Jun Zhao[a], Yuhang Liu[a], Guangfeng Li[a,*], Heng Wang[b], Yali Hou[c], Mingming Zhang[c], Xiaopeng Li[b], Xuzhou Yan[a,*]

[a] School of Chemistry and Chemical Engineering, Frontiers Science Center for Transformative Molecules, Shanghai Jiao Tong University, Shanghai 200240, China
[b] College of Chemistry and Environmental Engineering, Shenzhen University, Shenzhen 518055, China
[c] State Key Laboratory for Mechanical Behavior of Materials, Shaanxi International Research Center for Soft Matter, School of Materials Science and Engineering, Xi'an Jiaotong University, Xi'an 710049, China

ARTICLE INFO

Article history:
Received 6 October 2020
Received in revised form 8 December 2020
Accepted 14 December 2020
Available online 19 December 2020

Keywords:
Conformational effect
Structure-property relationship
Aggregation-induced emission
Coordination-driven self-assembly
Metallacycles

ABSTRACT

Herein, we designed and constructed two metallacycles, **1** and **2**, to illustrate the conformational effect of isomeric AIE fluorophores on the platform of supramolecular coordination complexes (SCCs). Specifically, the dangling phenyl rings in TPE units of the metallacycle **1** align completely outside the main cyclic structure, while in the metallacycle **2**, these phenyl rings align half inside and half outside. The experimental results showed that two metallacycles exhibited different behaviors in terms of AIE fluorescence and chemical sensing, which could be attributed to the subtle structural difference of the TPE units. This work represents the unification of topics such as self-assembly, AIE, and chemical sensing, and further promotes the understanding for the structure-property relationship of isomeric AIE fluorophores.

In recent years, fluorescent materials are undergoing accelerated and sustained growth. They have gained considerable attention due to widespread applications in environmental sensing, bioimaging, lighting devices and so on [1–4]. However, traditional fluorophores only work well in dilute conditions. The fluorescence would quench abruptly if they accumulate in the condensed phase, which is known as the frustrating aggregation-caused quenching (ACQ) phenomenon [5,6]. This troublesome problem was subtly tackled when Tang *et al*. reported an entirely opposite phenomenon called aggregation-induced emission (AIE) [7,8]. In this case, some typical chromophores emit faintly in dilute solutions but intensively in concentrated solutions. Such brand-new properties could be attributed to the restriction of intramolecular rotation and vibration of chromophores in the aggregated state. These AIE-active fluorogens bridged the gaps in traditional luminous materials, thus driving a huge bulk of researches [9–12]. Although sophisticated structures and delicate design of AIE molecules/assemblies have been reported [13–15], the relationship between the conformation of AIE units and the resulting photophysical properties has rarely been studied.

Supramolecular coordination complexes (SCCs), prepared by means of coordination-driven self-assembly, provide a suitable platform for further study of AIE chemistry [16,17]. Discrete metallacycle, a certain type of SCCs, can be efficiently achieved through self-assembly of ligands and central metals *via* labile coordination bonds. Were the angularities, directionalities, and stoichiometries defined, these building blocks would then contribute to the assumed exquisite structures through reversible bonds efficiently [18–21]. Owing to their controllable structures and properties, the detailed structure-property relationship of AIE moieties could be explored at the (supra)molecular level. Tetraphenylethylene (TPE) group is one of the most frequently used AIE units due to its facile synthesis and excellent stability [22,23]. Its original free rotation of phenyl rings and double bond could be restricted in the aggregated state, thus leading to the emission of fluorescence. After being fabricated by pyridine groups, TPE ligands could be implanted in the SCC systems. In recent years, we have reported the construction of light-emitting metal-organic materials on the SCC platforms and then investigated the influence on their AIE performance in terms of shapes, counter anion, number of chromophores and so on [24].

However, the relationship between the fine structure of AIE units and the corresponding fluorescence remains unsettled. It is plausible that any fine modulation may bring about a profound

* Corresponding authors.
E-mail addresses: guangfengli@sjtu.edu.cn (G. Li), xzyan@sjtu.edu.cn (X. Yan).

https://doi.org/10.1016/j.cclet.2020.12.028

influence on the fluorescent behavior, resulting from the difference of rotating restriction. For example, the more confined a TPE molecule is, the more salient AIE behavior it would display.

Herein, we designed two similar metallacycles, **1** and **2**, with different conformations of TPE groups *via* coordination-driven self-assembly. In the structure of **1**, the dangling phenyl rings are totally aligned outside of the core of metallacycle and the TPE units are restrained through two adjacent vertexes. While in the structure of **2**, only half of the dangling phenyl rings are outside and the other half are inside the metallacycle. The TPE units are restrained through two opposite vertexes, which make TPE units rotate or vibrate more restrictively. The key principle in our design is to ensure that, with the metal acceptors and counterpart anions being the same, the only difference of two metallacycles lies in the conformation of the TPE units. It is logically predicable that these two metallacycles would show different light-emitting behaviors which are worthy of investigation in detail.

In this study, we combined two different 0° TPE-based dipyridyl ligands **4** and **5**, and a di-Pt(II) acceptor **3**, to construct metallacycles **1** and **2**, respectively. Ligands **4** and **5** were readily prepared by Suzuki coupling and further purified. The mixture of di-Pt(II) acceptor **3** with ligand **4** or **5** in a 1:1 ratio was stirred in CD_2Cl_2 at room temperature for 8 h, and thus two self-assembled metallacycles **1** and **2**, were formed, respectively (Fig. 1).

Metallacycles **1** and **2** displayed a similar characteristic in the ^{1}H NMR spectra (Figs. 2a-f). All the hydrogen protons of the pyridine and phenyl rings exhibited downfield shifts to various degrees compared to those of original TPE ligands and Pt(II) acceptor. The peaks corresponding to the pyridine rings downfield shift by a large margin owing to the loss of electron density after metal-coordination. The ^{31}P{^{1}H} NMR spectra of **3**, **1**, and **2**, displayed sharp singlets (*ca.* 19.03 ppm for **3**, 12.84 ppm for **1**, and 12.86 ppm for **2**) with concomitant ^{195}Pt satellites in correspondence to a single phosphorus environment (Figs. 2g–i). The peaks of metallacycles **1** and **2** are shifted upfield from the di-Pt(II) acceptor by approximately 6.19 and 6.17 ppm, respectively, due to the electron backdonation effect of the Pt centers. Meanwhile, the coupling of the lateral ^{195}Pt satellites decreased (*ca.* $\Delta J = -164.0$ Hz for **1**, $\Delta J = -154.5$ Hz for **2**) due to the same electron back-donation effect. It was worth noting that the chemical shifts of **1** and **2** are very close, which implies two phosphorus ligands in different metallacycles were in similar environments. The clear-cut signals in both ^{31}P{^{1}H} and ^{1}H NMR spectra of these species together with the favorable solubility actively support the molecularity of these dual-TPE metallacycles.

Electrospray ionization time-of-flight mass spectrometry (ESI-TOF-MS) is an efficient and reliable tool for confirmation of the stoichiometry of multi-charged supramolecular species. The ESI-TOF-MS characterizations further convinced the existence of dual-TPE metallacycles **1** and **2**. In the mass spectrum of **1**, three peaks assigned demonstrate the formation of a [2 + 2] assembly (Figs. S7 and S10 in Supporting information). These peaks corresponded to the intact entity with different numbers of remaining counterions (m/z = 712.27 for $[M–4OTf]^{4+}$, m/z = 1000.00 for $[M–3OTf]^{3+}$ (Fig. 2j), m/z = 1573.50 for $[M–2OTf]^{2+}$, where M represents the intact assembly). Given metallacycle **2** has the same molecular weight with **1**, its fragments were similar to those in **1** (m/z = 712.26 for $[M–4OTf]^{4+}$, m/z = 1000.02 for $[M–3OTf]^{3+}$ (Fig. 2k), m/z = 1573.50 for $[M–2OTf]^{2+}$). All the assigned peaks have been isotopically resolved and were consistent with their computational distributions, indicating the formation of discrete metallacycle structure.

Due to the highly regular structure, the metallacycle **1** could pile up compactly, and therefore it is relatively easy to grow single crystals. As to the metallacycle **2**, however, providing that the benzene rings were half inside and half outside, metallacycles were difficult to get close to each other and the process of accumulation was hindered. Therefore, many methods applied were failed to grow single crystals suitable for X-ray scattering. The crystal structure of metallacycle **1** was displayed in the Fig. 2l with

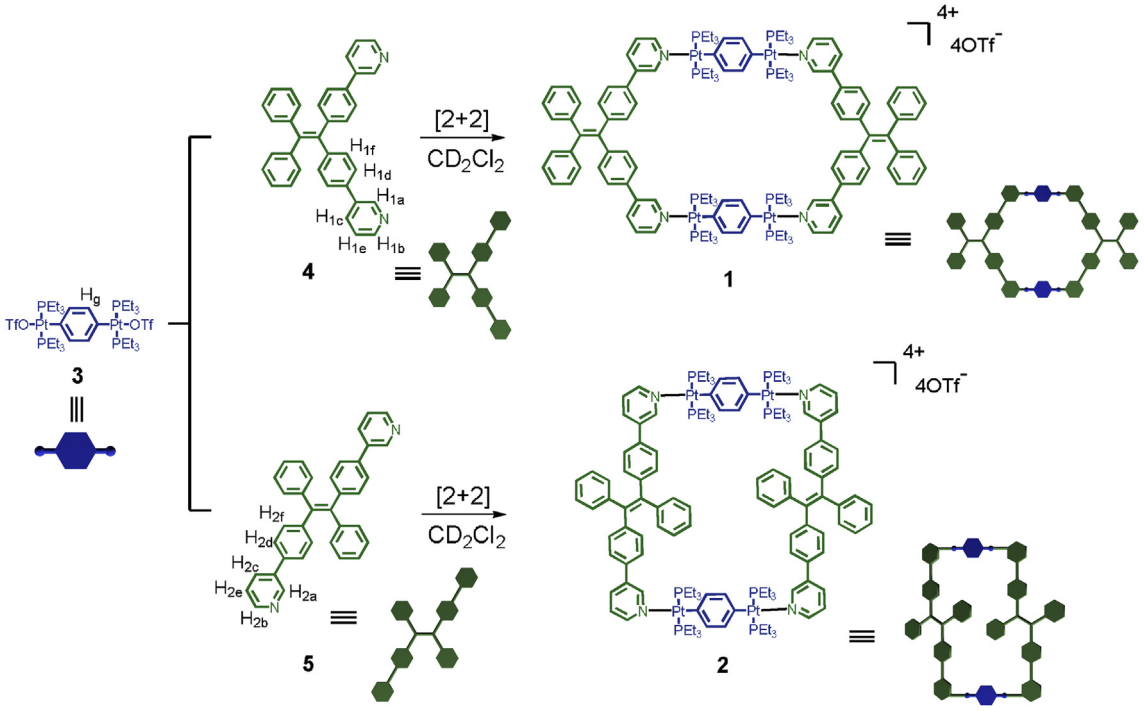

Fig. 1. Schematic representation of the formation of metallacycles **1** and **2** *via* coordination-driven self-assembly.

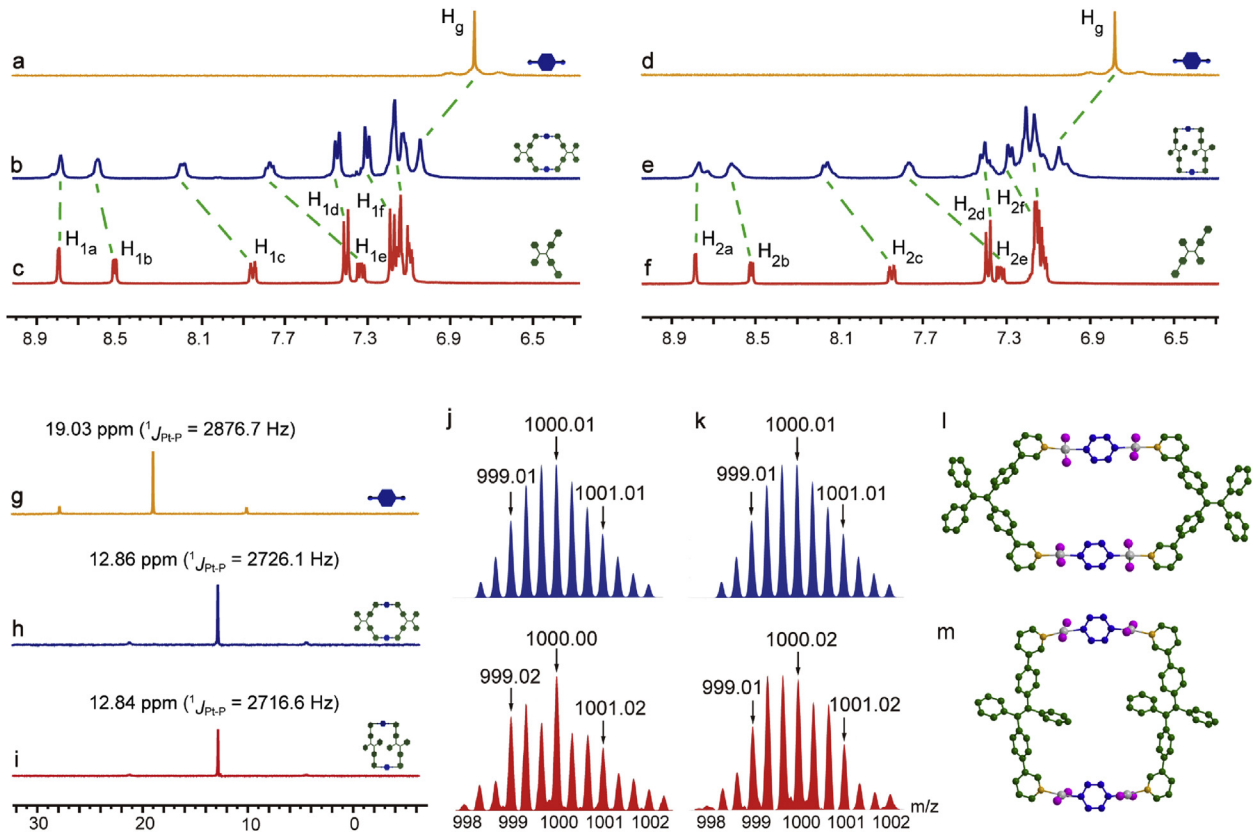

Fig. 2. Partial ^{1}H NMR spectra (400 MHz, CD_2Cl_2, 293 K) (a–f) and $^{31}P\{^1H\}$ spectra (161.9 MHz, CD_2Cl_2, 293 K) (g–i) of ligands **4** (c), **5** (f), acceptor **3** (a, d and g), metallacycles **1** (b, h), and **2** (e, i). Experimental (red) and calculated (blue) ESI-TOF-MS spectra of **1** $[M–3OTf]^{3+}$ (j) and **2** $[M–3OTf]^{3+}$ (k). Ball–stick views of the X-ray structure of metallacycle **1** (l) and optimized (B3LYP/6-31G(d, p)) structure of metallacycle **2** (m). Carbon atoms of ligands **4** and **5** are green, carbon atoms of acceptor **3** are blue, nitrogen atoms are yellow, phosphorus atoms are purple, and platinum atoms are grey. Hydrogens and counterions OTf^- (trifluoromethanesulfonate) anions are omitted for clarity.

counterions and ethyl groups removed for clarity. Instead, a DFT calculation was carried out to further understand the structure of metallacycle **2** (Fig. 2m). Both the single-crystal of **1** and the molecular simulation of **2** showed very similar, roughly planar structure. Their similar frameworks laid a solid foundation that different luminous behaviors could be attributed to the TPE conformation.

The normalized absorption spectra of ligands **4**, **5** and metallacycles **1**, **2** are shown in Fig. 3a. Ligands **4** and **5** exhibited a broad absorption band centered at 300 and 325 nm, respectively. After coordination, the absorption band of **1** displayed a red-shifted to 316 nm while **2** red-shifted to 331 nm, compared to relative ligands. The fluorescence emission spectra of ligands **4** and **5** as well as metallacycles **1** and **2** were also measured (Fig. 3b). Ligands **4** and **5** both exhibited a broad band and were weakly emissive at *ca.* 454 and 462 nm in CH_2Cl_2 at room temperature, respectively. The relatively low emission was attributed to the non-radiative relaxation pathway *via* intramolecular rotations of the phenyl and pyridyl rings. After the metallacycles were assembled, the emission intensity enhanced by a large scale. Both metallacycles **1** and **2** displayed single bands with maximum emission wavelength red-shifted to 476 and 508 nm, respectively. According to the fluorescent mechanism, a coplanar phenyl ring promoting π-electron conjugation contributes to hyperchromic effect while a perpendicular conformation weakening π-electron conjugation results in a blue shift. Consequently, a given emission wavelength shift is oftentimes related to a definite conformation of the phenyl rings. The phenyl rings in metallacycle **1** are not as rigid or conjugated as those in **2**, which makes the metallacycle **1** possess an enhanced redshift spectrum. In both metallacycles, the fluorescence enhancement was yet limited, suggesting that the TPE units are not hardened adequately to eliminate the non-radiative relaxation pathways.

In order to study the AIE properties of metallacycles **1** and **2**, the emission spectra were recorded in CH_2Cl_2 and CH_2Cl_2/hexane mixed solutions. In dilute CH_2Cl_2 solutions (Figs. 3c and d), the fluorescence of **1** was exceedingly weak and the emission intensity remained low in mixed solutions when the hexane content was less than 60%. In sharp contrast, when the hexane content increased to 90%, the fluorescence intensity increased overwhelmingly. It is presumable that the pendant phenyl rings which provided non-radiative relaxation pathways became rigid upon aggregation, resulting in apparent emission enhancement. Accordingly, metallacycle **2** displayed a similar AIE phenomenon (Figs. 3e and f). It was not until the hexane fraction reached 60% that the emission intensity remained inconspicuous. Their behavior in mixed solutions indicated both of the metallacycles were AIE-active. Yet some subtle differences could be found in two metallacycles. The structure with half phenyl rings inside in the metalacyclic skeleton probably brought about a decrease in solubility, which ultimately interpreted that aggregation started to occur at a lower percentage of hexane compared to that of metallacycle **1**.

The quantum yields of the two metallacycles were recorded in solvent medium as well as in solid-state. In dilute CH_2Cl_2 solution (c = 10.0 μmol/L), the quantum yield of metallacycle **1** was measured to be 0.17% while metallacycle **2** was measured to be 0.67%. The weak emission in solvent was owing to the slight

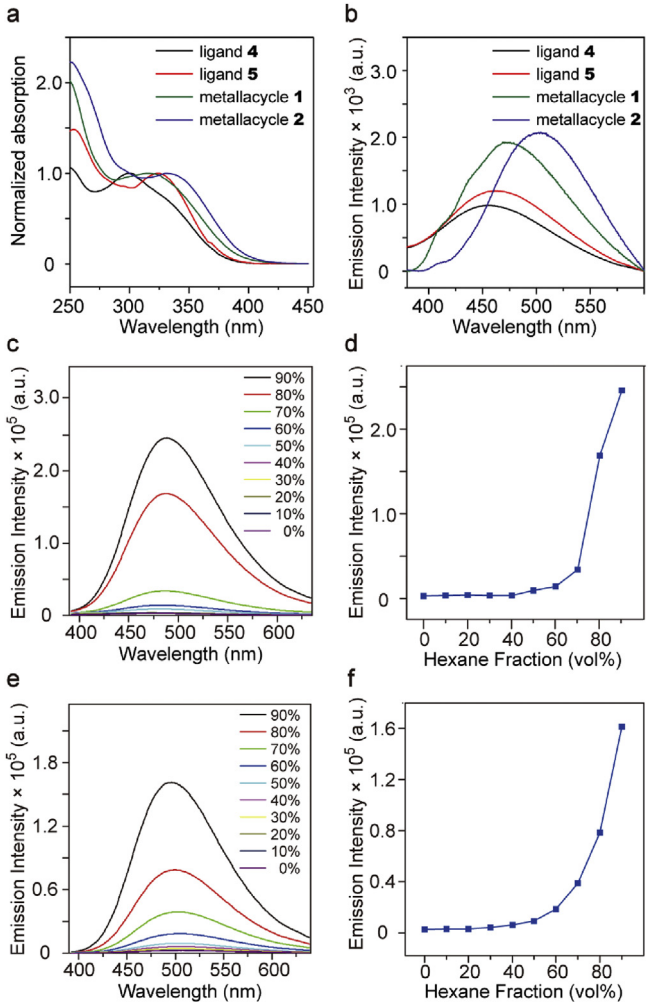

Fig. 3. Absorption (a) and fluorescence emission (b) spectra of ligands **4** and **5**, and metallacycles **1** and **2** in CH_2Cl_2. Fluorescence emission spectra and plots of maximum emission intensity of metallacycles **1** (c,d) and **2** (e,f) *versus* hexane fraction in CH_2Cl_2/hexane mixtures (λ_{ex} = 350 nm, c = 10.0 μmol/L).

restriction of intramolecular rotation of TPE units in the metallacycles. And in the solid state, the Φ_F values of **1** and **2** reached 24% and 33%, respectively. Notably, the *trans*-metallacycle **2** displayed higher Φ_F value than that of *cis*-metallacycle **1**. It is reasonable that the rigid structure of **2** with half phenyl rings inside restricts TPE units more tightly, and this restriction was enhanced when in the concentrated state. On the contrary, **1** showed relatively poorer fluorescent performance both in dilute solutions and in the solid state since the rotation of the phenyl rings is not highly restrained. The distinct difference between quantum yields suggests that the conformation of fluorogens has a considerable influence on the luminous properties of TPE-based metal-organic materials.

It has been reported that TPE-based metallacycles could act as chemosensors for nitroaromatic molecules and the detection sensitivity is related to the fine structure of metallacycle. Herein, we utilized picric acid (PA) as a typical nitroaromatic molecule to measure the potential sensing abilities of metallacycles **1** and **2**. The aggregated complexes in the 90% hexane content of CH_2Cl_2/hexane mixture were considered as turn-off fluorescent probes. Generally, emission intensity becomes attenuated in response to PA addition on account of a static quenching mechanism. Hence, the quenching processes could be monitored by the change of emission intensity. As is shown in Figs. 4a and b, the fluorescence quenching was distinctly observed even the PA concentration was as low as 0.1 μg/mL or 0.1 ppm, which is comparable to the related reports [25]. When the PA concentration kept increasing, the fluorescence decreased correspondingly. Even though two metallacycles have similar structures, **2** did not show the same extent of quenching efficiency of **1**. To conduct semi-quantitative analysis, we applied a linear Stern-Volmer equation I_0/I = K[PA] + 1 [26]. By means of linear fitting, the quenching constants K of the two metallacycles were calculated to be 6.13×10^4 L/mol for **1** and 3.51×10^4 L/mol for **2** (Fig. 4c). It is plausible that metallacycle **2**, with crowded steric effect, may hamper the approach of PA molecules to form nonemissive ground-state complexes.

In summary, we have not only synthesized and characterized two dual-TPE-based metallacycles, but also used the metallacycles as the platform to study the relationship between conformations of the TPE units and corresponding photophysical properties. In detail, two metallacycles, **1** and **2**, were constructed by virtue of coordination driven self-assembly. In metallacycle **1**, TPE units were totally arranged outside. The metallacycle **2** had half TPE units embedded within the metallacycle, leaving TPE groups in a more constrained conformation. During molecular aggregation, two metallacycles experienced marked fluorescence enhancement. Given the metallacycle **2** in a more constrained state, it behaved more apparent AIE behavior and owned a higher quantum yield. Moreover, the two metallacycles exhibited highly sensitive to picric acid. These findings provide an extensive understanding of the influence of the fine structure of AIEgens on the fluorescent properties as well as sensing applications of AIE-active metallacycles.

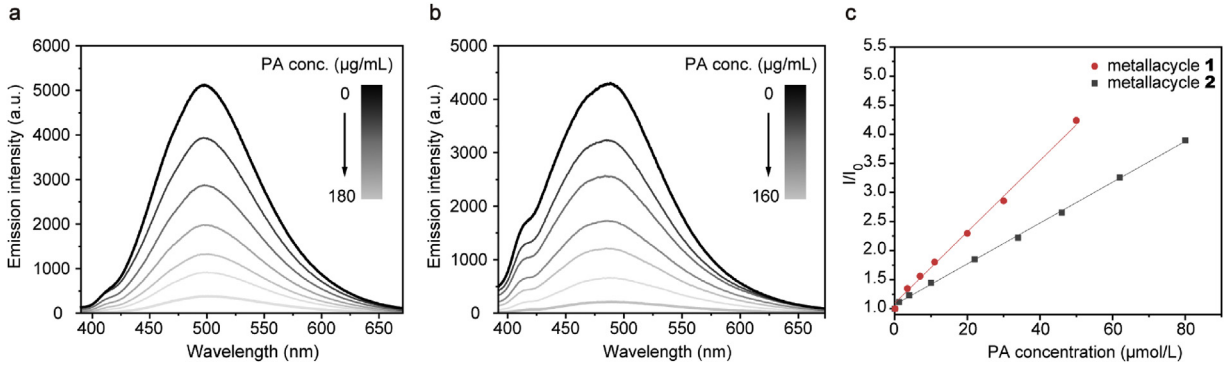

Fig. 4. Fluorescence emission spectra of metallacycles **1** (a) and **2** (b) in 10%/90% CH_2Cl_2/hexane mixture containing different amounts of picric acid (PA) (λ_{ex} = 350 nm, c = 10.0 μmol/L). (c) Plot of relative fluorescence intensities (I_0/I, I = peak intensity and I_0 = peak intensity at [PA] = 0 μmol/L) *versus* picric acid concentrations in 10%/90% CH_2Cl_2/hexane mixture (λ_{ex} = 350 nm, c = 10.0 μmol/L).

Declaration of competing interest

The authors declare that they have no known competing financial interests or personal relationships that could have appeared to influence the work reported in this paper.

Acknowledgments

This work was financially supported by the National Natrual Science Foundation of China (Nos. 21901161 and 22071152), Natural Science Foundation of Shanghai (No. 20ZR1429200), the China Postdoctoral Science Foundation (No. 2020M671094), and Basic Research Program of Xi'an Jiaotong University (No. XZY022020018).

Appendix A. Supplementary data

Supplementary material related to this article can be found, in the online version, at doi:https://doi.org/10.1016/j.cclet.2020.12.028.

References

[1] B. Li, M. Zhao, L. Feng, et al., Nat. Commun. 11 (2020) 3102.
[2] Y. Ma, C. Yan, Z. Guo, et al., Angew. Chem. Int. Ed. 59 (2020) 9812–9825.
[3] M. Zuo, W. Qian, M. Hao, et al., Chin. Chem. Lett. (2020), doi:http://dx.doi.org/10.1016/j.cclet.2020.09.033.
[4] Z. Zhou, D.G. Chen, M.L. Saha, et al., J. Am. Chem. Soc. 141 (2019) 5535–5543.
[5] S.M. Borisov, O.S. Wolfbeis, Chem. Rev. 108 (2008) 423–461.
[6] R.T. Kwok, C.W. Leung, J.W. Lam, B.Z. Tang, Chem. Soc. Rev. 44 (2015) 4228–4238.
[7] J. Luo, Z. Xie, J.W. Lam, et al., Chem. Commun. 18 (2001) 1740–1741.
[8] J. Mei, N.L.C. Leung, R.T.K. Kwok, J.W.Y. Lam, B.Z. Tang, Chem. Rev. 115 (2015) 11718–11940.
[9] J. Li, J. Wang, H. Li, et al., Chem. Soc. Rev. 49 (2020) 1144–1172.
[10] Y. Li, Y. Dong, X. Miao, et al., Angew. Chem. Int. Ed. 130 (2018) 737–741.
[11] X. Yan, P. Wei, Y. Liu, et al., J. Am. Chem. Soc. 141 (2019) 9673–9679.
[12] W. Qian, M. Zuo, G. Sun, et al., Chem. Commun. 56 (2020) 7301–7304.
[13] J.L. Zhu, L. Xu, Y.Y. Ren, et al., Nat. Commun. 10 (2019) 4285.
[14] B. Li, T. He, Y. Fan, et al., Chem. Commun. 55 (2019) 8036–8059.
[15] G. Li, L. Wang, L. Wu, et al., J. Am. Chem. Soc. 142 (2020) 14343–14349.
[16] X. Yan, T.R. Cook, P. Wang, F. Huang, P.J. Stang, Nat. Chem. 7 (2015) 342–348.
[17] M.L. Saha, X. Yan, P.J. Stang, Acc. Chem. Res. 49 (2016) 2527–2539.
[18] Z. Zhang, Y. Li, B. Song, et al., Nat. Chem. 12 (2020) 468–474.
[19] Y. Inomata, T. Sawada, M. Fujita, Chem 6 (2020) 294–303.
[20] Z. Wang, L. He, B. Liu, et al., J. Am. Chem. Soc. 142 (2020) 16409–16419.
[21] G. Li, Z. Zhou, C. Yuan, et al., Angew. Chem. Int. Ed. 59 (2020) 10013–10017.
[22] G.Q. Yin, H. Wang, X.Q. Wang, et al., Nat. Commun. 9 (2018) 567.
[23] L.Z. Ma, T.F. Yang, Z.Y. Zhang, et al., Chin. Chem. Lett. 30 (2019) 1942–1946.
[24] X. Yan, M. Wang, T.R. Cook, et al., J. Am. Chem. Soc. 138 (2016) 4580–4588.
[25] X. Yan, H. Wang, C.E. Hauke, et al., J. Am. Chem. Soc. 137 (2015) 15276–15286.
[26] J. Liu, Y. Zhong, P. Lu, et al., Polym. Chem. 1 (2010) 426–429.